Temporal quantum correlations in inelastic light scattering from water

Author(s):
Kasperczyk, Mark; de Aguiar Júnior, Filomeno S.; Rabelo, Cassiano; Saraiva, André; Santos, Marcelo F.; Novotny, Lukas; Jório, Ado

Publication date:
2016-12-09

Permanent link:
https://doi.org/10.3929/ethz-a-010807096

Originally published in:
Physical Review Letters 117(24), https://doi.org/10.1103/PhysRevLett.117.243603

Temporal Quantum Correlations in Inelastic Light Scattering from Water

Mark Kasperczyk,[1] Filomeno S. de Aguiar Júnior,[2] Cassiano Rabelo,[3] Andre Saraiva,[4] Marcelo F. Santos,[4] Lukas Novotny,[1] and Ado Jorio[2,*]

[1]*Photonics Laboratory, ETH Zürich, 8093 Zürich, Switzerland*

[2]*Departamento de Física, Universidade Federal de Minas Gerais, Belo Horiztone, Minas Gerais 31270-901, Brazil*

[3]*Programa de Pós-Graduação em Engenharia Elétrica, Universidade Federal de Minas Gerais, Belo Horiztone, Minas Gerais 31270-901, Brazil*

[4]*Instituto de Física, Universidade Federal do Rio de Janeiro, Rio de Janeiro, Rio de Janeiro 21941-972, Brazil*

(Received 24 June 2016; published 7 December 2016)

Water is one of the most prevalent chemicals on our planet, an integral part of both our environment and our existence as a species. Yet it is also rich in anomalous behaviors. Here we reveal that water is a novel—yet ubiquitous—source for quantum correlated photon pairs at ambient conditions. The photon pairs are produced through Raman scattering, and the correlations arise from the shared quantum of a vibrational mode between the Stokes and anti-Stokes scattering events. We confirm the nonclassical nature of the produced photon pairs by showing that the cross-correlation and autocorrelations of the signals violate a Cauchy-Schwarz inequality by over 5 orders of magnitude. The unprecedented degree of violating the inequality in pure water, as well as the well-defined polarization properties of the photon pairs, points to its usefulness in quantum information.

DOI: 10.1103/PhysRevLett.117.243603

Water has numerous anomalous properties [1]. It blankets over 70% of Earth's surface [2], and it is spread across the Universe, appearing in extrasolar planets [3]. We ourselves are more than 60% water [4], and nearly 70% of the water consumption on our planet goes toward agriculture [2,5]. Even the optical properties of this elementary liquid are surprisingly important, as water is a primary absorber of sunlight and thereby contributes to the stability of our climate [6].

Among optical processes, Raman scattering is relevant in providing a vibrational fingerprint for chemicals, and it is especially interesting for generating quantum correlated photon pairs [7–9]. Compared to other sources of instantaneous photon pairs studied for quantum information and quantum computing, such as spontaneous parametric down-conversion [10] or spontaneous four-wave mixing [11,12], the Stokes–anti-Stokes (SAS) correlated Raman scattering shows promise as a write-read protocol for quantum memory [9,13–15]. However, from all the materials already discovered as sources of the SAS correlated photons, including micromechanical devices, the degree of correlation has always been low compared to other sources of photon pairs, hindering the possibility of developing further applications from the SAS effect. Here we show that water at ambient conditions surpasses all the previous materials in SAS production purity by orders of magnitude, violating the Cauchy-Schwarz inequality by more than 5 orders of magnitude, which is unprecedented in quantum optics and materials science.

The correlations between the Stokes (S) and anti-Stokes (AS) photons arise from the fact that they share the same quantum of vibration: A laser pulse interacts with a water molecule to initiate a vibrational mode and generate a redshifted S photon; the same laser pulse then interacts with the newly created vibration to generate a blueshifted AS photon. We exploit the two main Raman features from liquid water to produce photon pairs in ambient conditions (see Fig. 1), specifically one Raman band at 1640 cm^{-1} (ν_2 symmetric bending mode) and one at 3400 cm^{-1} (comprising the symmetric ν_1 and antisymmetric ν_3 stretching modes, plus the combination $2\nu_2$) [16]. Both bands are capable of producing nonclassical photon pairs.

To prove that the S and AS photons we measure from water are indeed a temporally correlated quantum pair, we must examine a version of the Cauchy-Schwarz inequality that applies to the cross-correlations. For classical sources of light, the cross-correlation $g^{(2)}_{S,AS}(0)$ is bound by the inequality $[g^{(2)}_{S,AS}(0)]^2 \leq g^{(2)}_{S,S}(0) \times g^{(2)}_{AS,AS}(0)$, where $g^{(2)}_{S,S}(0)$ is the autocorrelation of the Stokes signal, and similarly for $g^{(2)}_{AS,AS}(0)$ [18]. Classically, the cross- and autocorrelations can be written in terms of the instantaneous intensities of the fields, representing their statistical properties. A quantum treatment, however, requires quantizing the fields and writing the correlations in terms of the photon creation and annihilation operators [18,19]. Since the quantum treatment is not bound by the above inequality, violating it indicates quantum behavior of the measured fields.

We measure the cross-correlation through a time-correlated single-photon counting system. A 0.5 NA objective focuses the light of a pulsed excitation laser (pulse duration 200 fs and wavelength 633 nm) into a sample container filled with distilled liquid water, with an average

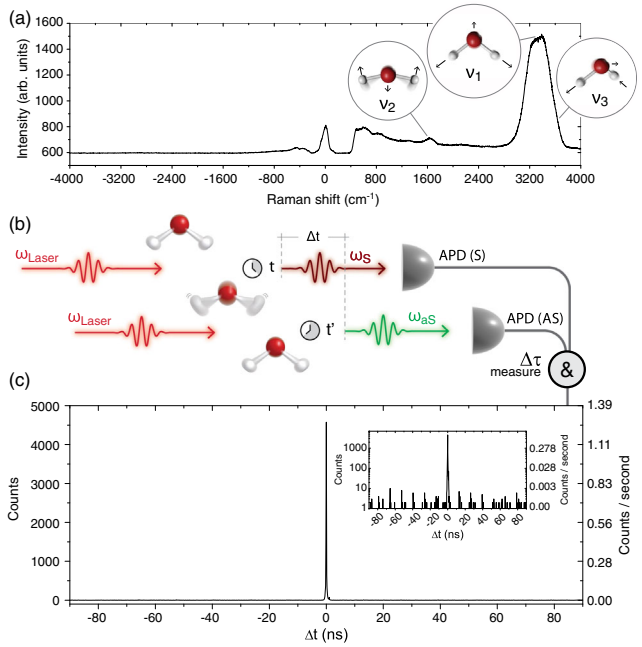

FIG. 1. (a) S(+) and AS(−) Raman spectrum of liquid water, including the three intramolecular H_2O vibrations (ν_1, ν_2, and ν_3; see the schematics). The spectrometer charge coupled device camera is not capable of distinguishing the AS signal from the readout noise in this 1h-accumulation spectrum. Intermolecular vibrations appear at lower frequencies [16], and the peak at zero is leakage from laser through the notch filter (cuts from −200 up to +400 cm^{-1}). These unwanted signals are removed in the temporal correlation measurements by bandpass filters [17]. (b) Schematics explaining the production of correlated photons within the ν_2 mode. In the S process, at time t, an incident photon from the laser (ω_{laser}) is converted into a photon with smaller energy (ω_S), and the remaining energy is transferred to the molecule as a quantum of vibration. At time t', another photon from the laser is converted into a photon with higher energy (ω_{AS}) in the AS process by absorbing the quantum of vibration. The time for the energy exchange between S and the AS processes is shown by $\Delta t = t' - t$. (c) Histogram of measured Δt values from ν_2. The corresponding cross-correlation function at zero delay is $g^{(2)}_{S,AS}(0) = 915$, the highest value we achieved. The signal (peak at $\Delta t = 0$) is 3 orders of magnitude higher than the background (peaks at $\Delta t \neq 0$); see the inset [17].

laser power of ∼19 mW, corresponding to ∼250 pJ per pulse. The path length through the water is ∼1 mm. A 0.9 NA objective collects the S and AS scattered light in transmission. Correlations are measured in a forward scattering geometry [13]. A notch filter blocks the excitation light, and a pinhole blocks unwanted background light. For cross-correlation measurements, a dichroic beam splitter separates the S and AS beams, sending them to separate single-photon counting avalanche photodiodes (APDs). Bandpass filters in front of each APD block any remaining light (see the schematics for the experimental setup in Ref. [17]), except for photoluminescence (PL) that overlaps with the Stokes Raman peak. PL photons do not contribute to our coincidence measurements, since they appear only in the Stokes spectral region [see Fig. 1(a)].

The arrival times of the S and AS photons at the APDs are recorded by a time-correlated single-photon counting system, which creates a histogram of the coincidences. The procedure compares the arrival times (Δt) of the detected photons and thereby builds a histogram of coincidences [see Figs. 1(b) and 1(c) and Ref. [17]]. Because the lifetimes of the vibrational modes (0.9 ps for the bending mode and 260 fs for the stretching mode [20,21]) are much shorter than the repetition time between consecutive laser pulses (13.2 ns), all correlated photon pairs must arise from within the same pulse. Therefore, normalizing the histogram by the number of accidental coincidences (i.e., the number of counts at $\Delta t = 0$ divided by the average of counts in the peaks at $\Delta t \neq 0$) yields an experimental measure of $g^{(2)}_{S,AS}(0)$. The finite time resolution of the measurement is dominated by the APD timing jitter (∼50–100 ps for each APD), and the full width at half maximum (FWHM) of the counting peaks adds up to 0.3 ns. Evaluating the impact of the timing jitter on the measured value of the cross-correlation shows that its impact is negligible [17,22].

For the ν_2 symmetric bending mode at 1640 cm^{-1}, we measured cross-correlation values as high as $g^{(2)}_{S,AS}(0) \sim 10^3$ [see Fig. 1(c) and inset]. To test the Cauchy-Schwarz inequality, we measured a cross-correlation value of $g^{(2)}_{S,AS}(0) = 653 \pm 54$, along with autocorrelation values of $g^{(2)}_{S,S}(0) = 0.7 \pm 0.2$ and $g^{(2)}_{AS,AS}(0) = 0.8 \pm 0.6$ (errors are an overestimation based on the limiting values observed for $\Delta t \neq 0$). For autocorrelation measurements, the dichroic is replaced by a 50:50 beam splitter, and either the S or the AS bandpass filter is placed before the beam splitter. Inserting these values into the Cauchy-Schwarz inequality shows that it is violated by 6 orders of magnitude, proving that the S and AS photons generated by water exhibit astonishing nonclassical correlations in arrival time.

The huge values of $g^{(2)}_{S,AS}(0)$ measured in water are to be compared to measured values found in other materials, including the range $g^{(2)}_{S,AS}(0) = 5$–33 measured in diamond (Refs. [13,23], and later in this work), the value of $g^{(2)}_{S,AS}(0) = 6$ reported in a Si-based micromechanical cavity [15], and the range $g^{(2)}_{S,AS}(0) = 2.3$–20 measured in gases [8,24,25], in which the atomic hyperfine structure is exploited rather than molecular vibrational levels [26–28]. These references discuss the possible implementation of quantum protocols based on the SAS phenomena, but, while accidental coincidences provide a significant yet surmountable contribution to the signal in all the previously measured systems, in water nearly every AS photon from the symmetric bending mode that reaches the detector comes from the SAS process, making accidental coincidences almost negligible.

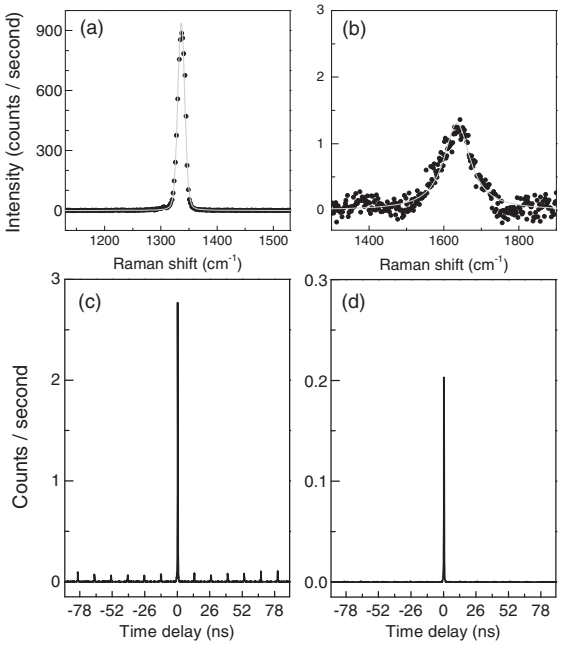

FIG. 2. (a) and (b) plot, respectively, the Raman spectra from diamond and the ν_2 bending mode of liquid water. (c) and (d) plot, respectively, the histogram of coincidences for diamond [$g^{(2)}_{S,AS}(0) = 33$] and for water [$g^{(2)}_{S,AS}(0) = 549$]. The uncertainties in all the measured cross-correlations and the spectra are due primarily to Poissonian noise in the photon counting [17]. (a) and (b) or (c) and (d) were measured with the same experimental apparatus for direct comparison.

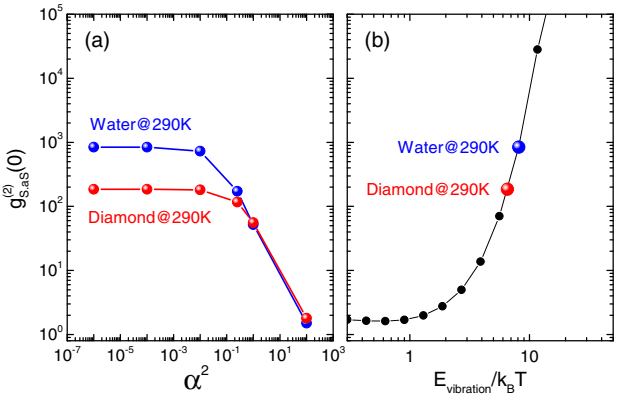

FIG. 3. (a) Calculated dependence of the SAS correlation [$g^{(2)}_{S,AS}(0)$] on the number of incident photons (α^2) [19], for water (blue) and diamond (red). (b) Low photon fluency saturation values as a function of the ratio between the vibrational energy and the thermal energy ($E_{vibration}/k_BT$). Calculations here are for $T = 290$ K. More details are in Refs. [17,19].

Figure 2 shows a comparison between the Raman spectral profile of diamond [Fig. 2(a)] and liquid water [Fig. 2(b)] and the respective histogram of SAS coincidences [Figs. 2(c) and 2(d)]. The diamond measurements were performed using the same experimental apparatus, using a 50 μm-thick high-purity diamond sample grown by chemical vapor deposition. Although the integrated area for the diamond Raman peak is about 90 times stronger than for water [see Figs. 2(a) and 2(b)], the number of observed coincidences per second at $\Delta t = 0$ is only 13.5 times higher for diamond, showing that photons of higher energies are more efficient in converting two laser photons into an SAS photon pair. However, the most striking result is the average value for coincidences in the peaks at $\Delta t \neq 0$. In most cases in the literature, as well as for the diamond measurement shown in Fig. 2(c), there is a considerable number of uncorrelated photon pairs, with the AS photon often originating from thermally generated vibrational modes. In water, this average value is very close to zero [see Fig. 2(d)].

Reference [19] introduced a general quantum optical approach to describe the generation of correlated SAS pairs. The SAS effect scales with the inverse number of incident photons, but its efficiency is limited at a low photon fluency by the existence of thermal excitations that can also be used to generate uncorrelated AS photons [see Fig. 3(a)]. This model allows us to investigate the role of different parameters, such as (i) the laser pulse duration, (ii) the pulse peak intensity, (iii) the vibrational mode lifetime, and (iv) the ratio between vibrational excitation energy $E_{vibration} = \hbar\nu$ and thermal energy k_BT, which enters the model through the Bose-Einstein distribution n_0 [17]. We find that parameters (i)–(iii) have no noticeable impact on the correlation function [17]. Figure 3(b) shows the calculated $g^{(2)}_{S,AS}(0)$ as a function of $E_{vibration}/k_BT$, indicating that parameter (iv) plays a major role in determining $g^{(2)}_{S,AS}(0)$.

The predicted value for $g^{(2)}_{S,AS}(0)$ in water shown in Fig. 3(b) is consistent with our experimental results. Recently, the SAS event has also been studied in a two-dimensional resonator based on graphene [29], where the C—C stretching frequency matches that of the ν_2 water mode, but hot luminescence produced too much background signal to permit a measure of $g^{(2)}_{S,AS}(0)$. The predicted value for $g^{(2)}_{S,AS}(0)$ in diamond shown in Fig. 3(b), however, is roughly one order of magnitude higher than the observed values. Within our theoretical framework, a temperature raise up to $T = 382$ K would explain the observed $g^{(2)}_{S,AS}(0) = 33$ in Fig. 2(c). However, other decoherence channels not considered in the model, e.g., elastic vibrational mode scattering, would also reduce $g^{(2)}_{S,AS}(0)$.

An important question is whether these photons can be used in entanglement experiments, where one of the most prominent forms is based on polarization selection [9,30]. Therefore, we examine the polarization dependence of the Raman cross-correlation in water. We insert two polarizers, one in the AS path and one in the S path. When both polarizers are parallel to the excitation polarization [Fig. 4(a)], the cross-correlation exhibits superbunching

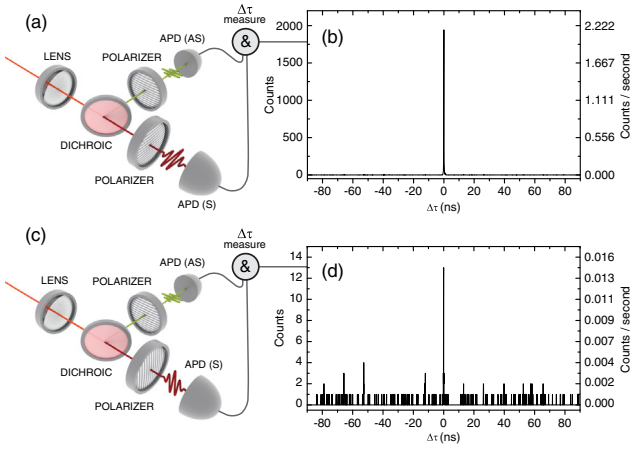

FIG. 4. Polarized nature of the 1640 cm^{-1} quantum correlated SAS emission from water. (a) Both polarizers are oriented parallel to the excitation electric field. (b) The correlation is largely unchanged and still shows highly nonclassical correlation. The measured value of the cross-correlation is $g^{(2)}_{S,AS}(0) = 513$. (c) The AS polarizer is parallel to the excitation, while the S polarizer is perpendicular. (d) The coincidence rate is very weak, and the measured value of the cross-correlation is at least 2 orders of magnitude smaller. The observed value of $g^{(2)}_{S,AS}(0) \sim 6$ can be attributed to leakage through the polarizers.

comparable to the correlations measured without any polarizers present [Fig. 4(b)]. When the AS polarizer is parallel to the excitation and the S polarizer is perpendicular [Fig. 4(c)], the correlation and coincidence rates drop precipitously [Fig. 4(d)]. This strongly suggests that the polarization of the AS photon is determined by the polarization of the emitted S photon, a condition for exploring entangled photons from water.

Additionally, we measured nonclassical correlations between the Stokes and anti-Stokes signals from the 3400 cm^{-1} Raman band of water. This mode is of particular interest in the study of many biological systems, because the molecular coordination and therefore the properties of the molecular vibrations in biological materials can change dramatically compared to the relatively free bulk molecules [31]. For example, recent research has detected the onset of breast cancer by examining the Raman signal from breast tissue cells: Healthy cells show no significant Raman signal from the 3400 cm^{-1} stretching mode, whereas cancerous cells do [32–34]. This difference is attributed to the interaction of the interfacial water molecules with small crevices and channels found in tissues. We measure the cross- and autocorrelations for the 3400 cm^{-1} stretching mode and find that the inequality is violated, with a measured cross-correlation of $g^{(2)}_{S,AS}(0)$ over 20. When comparing the results from the two Raman bands in water, there are differences in vibrational mode frequencies, lifetimes, and Raman scattering cross sections [19,35,36]. However, the main aspect in the lower $g^{(2)}_{S,AS}(0)$ at 3400 cm^{-1} is that this band does not come from a single vibrational mode but rather from a collection of modes, thus making the effect more complex, with uncertainty in specific mode contributions. Regardless, there are at least two distinct Raman processes in water that are each capable of producing nonclassical photon pairs, and the strength of these effects can be used as novel probes of biological systems, e.g., as detectors of cancerous cells.

The discovery of liquid water as a source of nonclassical photon pairs reveals new avenues for exploring fundamental questions of quantum optics as well as the potential of developing concrete sensing applications for quantum optics. The unparalleled degree of superbunching observed, combined with the chaotic nature of fluids at the molecular level, enables new questions to be studied, including the effect of phase transitions on the ability of a material to generate photon pairs. Yet water's importance in biology and chemistry makes this a discovery of interdisciplinary relevance. Water also acts as the representative example of liquids in general as sources of Raman correlated photons, suggesting that other liquids should be studied to determine new properties of the correlations, such as the effects of intermolecular interactions or the influence of contaminants within the solution.

The authors acknowledge Professors Carlos H. Monten and Belita Koiller, Dr. Carlos A. Parra-Murillo, and Dr. Carolina Garin for fruitful discussions and Professor Patrick Maletinsky and Dr. Elke Neu for the diamond sample. Financial support: Conselho Nacional de Desenvolvimento Científico e Tecnológico (CNPq) (Grants No. 552124/2011-7, No. 305384/2015-5, and No. 309861/2015-2), Financiadora de Estudos e Projetos (Grant No. 01.13.0330.00), and the Swiss Nacional Centre of Competence in Research (NCCR)—Quantum Science and Technology (QSIT) program (Grant No. 51NF40-160591). M. K. acknowledges CNPq (Grant No. 552124/2011-7) for financing his visit to the Universidade Federal de Minas Gerais (UFMG).

*adojorio@fisica.ufmg.br

[1] K. Amann-Winkel, R. Böhmer, F. Fujara, C. Gainaru, B. Geil, and T. Loerting, Rev. Mod. Phys. **88**, 011002 (2016).
[2] I. A. Shiklomanov, in *Water in Crisis: A Guide to the World's Fresh Water Resources*, edited by P. H. Gleick (Oxford University Press, New York, 1993), Chap. 2.
[3] G. Tinetti *et al.*, Nature (London) **448**, 169 (2007).
[4] H. H. Mitchell, T. S. Hamilton, F. R. Steggerda, and H. W. Bean, J. Biol. Chem. **158**, 625 (1945).
[5] *Vital Water Graphics: An Overview of the State of the World's Fresh and Marine Waters*, 2nd ed. (United Nations Environment Programme, Nairobi, Kenya, 2008).
[6] R. A. McClatchey, R. W. Fenn, J. E. A. Selby, F. E. Volz, and J. S. Garing, *Optical Properties of the Atmosphere*,

3rd ed. (Air Force Cambridge Research Labs, Hanscom AFB, MA, 1972), accession number AD0753075.
[7] D. N. Klyshko, Sov. J. Quantum Electron. **7**, 755 (1977).
[8] A. Kuzmich, W. P. Bowen, A. D. Boozer, A. Boca, C. W. Chou, L.-M. Duan, and H. J. Kimble, Nature (London) **423**, 731 (2003).
[9] K. C. Lee *et al.*, Science **334**, 1253 (2011).
[10] K. Akiba, K. Kashiwagi, M. Arikawa, and M. Kozuma, New J. Phys. **11**, 013049 (2009).
[11] J. Fan, A. Migdall, and L. J. Wang, Opt. Lett. **30**, 3368 (2005).
[12] L. J. Wang, C. K. Hong, and S. R. Friberg, J. Opt. B **3**, 346 (2001).
[13] K. C. Lee, B. J. Sussman, M. R. Sprague, P. Michelberger, K. F. Reim, J. Nunn, N. K. Langford, P. J. Bustard, D. Jaksch, and I. A. Walmsley, Nat. Photonics **6**, 41 (2012).
[14] D. G. England, P. J. Bustard, J. Nunn, R. Lausten, and B. J. Sussman, Phys. Rev. Lett. **111**, 243601 (2013).
[15] R. Riedinger, S. Hong, R. A. Norte, J. A. Slater, J. Shang, A. G. Krause, V. Anant, M. Aspelmeyer, and S. Gröblacher, Nature (London) **530**, 313 (2016).
[16] G. E. Walrafen, J. Chem. Phys. **40**, 3249 (1964).
[17] See Supplemental Material at http://link.aps.org/supplemental/10.1103/PhysRevLett.117.243603 for (i) further details about the experimental setup, (ii) an explanation for the processes building the coincidence histogram, (iii) a theoretical description of the SAS rate, and (iv) a theoretical description of the coincidence statistics and error estimation.
[18] R. Loudon, *The Quantum Theory of Light* (Oxford University Press, New York, 2010).
[19] C. A. Parra-Murillo, M. F. Santos, C. H. Monken, and A. Jorio, Phys. Rev. B **93**, 125141 (2016).
[20] J. C. Deák, S. T. Rhea, L. K. Iwaki, and D. D. Dlott, J. Phys. Chem. A **104**, 4866 (2000).
[21] A. J. Lock and H. J. Bakker, J. Chem. Phys. **117**, 1708 (2002).
[22] M. M. Hayat, S. N. Torres, and L. M. Pedrotti, Opt. Commun. **169**, 275 (1999).
[23] M. Kasperczyk, A. Jorio, E. Neu, P. Maletinksy, and L. Novotny, Opt. Lett. **40**, 2393 (2015).
[24] V. Balić, D. A. Braje, P. Kolchin, G. Y. Yin, and S. E. Harris, Phys. Rev. Lett. **94**, 183601 (2005).
[25] M. Bashkansky, F. K. Fatemi, and I. Vurgaftman, Opt. Lett. **37**, 142 (2012).
[26] Z.-S. Yuana, X.-H. Bao, C.-Y. Lu, J. Zhang, C.-Z. Peng, and J.-W. Pan, Phys. Rep. **497**, 1 (2010).
[27] L.-M. Duan, M. D. Lukin, J. I. Cirac, and P. Zoller, Nature (London) **414**, 413 (2001).
[28] N. Sangouard, C. Simon, H. de Riedmatten, and N. Gisin, Rev. Mod. Phys. **83**, 33 (2011).
[29] A. Jorio, M. Kasperczyk, N. Clark, E. Neu, P. Maletinsky, A. Vijayaraghavan, and L. Novotny, Nano Lett. **14**, 5687 (2014).
[30] E. Y. Zhu, Z. Tang, L. Qian, L. G. Helt, M. Liscidini, J. E. Sipe, C. Corbari, A. Canagasabey, M. Ibsen, and P. G. Kazansky, Phys. Rev. Lett. **108**, 213902 (2012).
[31] M. Lafleur, M. Pigeon, M. Pézolet, and J.-P. Caillé, J. Phys. Chem. **93**, 1522 (1989).
[32] H. Abramczyk, J. Surmacki, B. Brożek-Płuska, Z. Morawiec, and M. Tazbir, J. Mol. Struct. **924–926**, 175 (2009).
[33] H. Abramczyk, B. Brożek-Płuska, J. Surmacki, J. Jablonska-Gajewicz, and R. Kordek, J. Biophys. Chem. **2**, 158 (2011).
[34] J. Surmacki, J. Musial, R. Kordek, and H. Abramczyk, Mol. Cancer **12**, 48 (2013).
[35] H. W. Schrötter, in *Infrared and Raman Spectroscopy: Methods and Applications*, edited by B. Schrader (VCH, Weinheim, 1995), Chap. 4.
[36] H. W. Schrötter and H. W. Klöckner, in *Raman Spectroscopy of Gases and Liquids*, edited by A. Weber, Topics in Current Physics Vol. 11 (Springer-Verlag, Berlin, 1979), Chap. 4.